Modelling and Analysis of A 6-DOF Robotic Arm for Oil and Gas Pipeline Welding Operations

B.E. Nyong-Bassey* and A.M. Epemu

Department of Electrical/Electronic Engineering, Federal University of Petroleum Resources Effurun, Nigeria

Abstract: Recent advances in robotics and automation technology have spurred the widespread use of robotic arms for industrial operations. Consequently, practising engineers, key players and particularly engineering students must be encouraged to stay abreast with these recent trends by developing hands-on and simulation experience. Therefore, this paper concisely presents the modelling, kinematic analysis as well as simulation results of an educational 6-DoF (Degrees of Freedom) robotic arm designed for welding oil and gas pipelines and other generalised tasks in a MATLAB/Simulink-Simscape environment. The joint movements of the robotic arm were simulated with a sinusoidal reference signal consisting of unit magnitude and frequency of 1 rad/s using the MATLAB Robotics Toolbox. Consequently, the results indicated satisfactory performance as the design allows the robot joints to effectively move the end-effector welding tool-piece in an elliptical path as would be required in the case of welding a cylindrical pipeline for oil and gas operations.

Keywords: Robotic automation, Manipulator, Modelling, Kinematics, 6-DoF, Welding, D-H.

1. INTRODUCTION

Over the last few decades, industrial robotic arms have been effectively perfected and particularly in areas where human abilities are limited, robotic manipulators can easily maintain remote control for operators. A robotic arm is a mechanical system that looks like a human arm but can be programmed to perform different tasks [1].

Ali *et al*. [1] designed a pair of 6-DOF robot manipulator models to address the existing issue of advancing 3D printing in construction engineering. One of the robots was responsible for transporting construction materials, while the other is responsible for printing building blocks and walls with concrete mixtures using an end effector. For the proposed designs, the mathematical model of the robot manipulator was driven by the principles of forward and inverse kinematics. Later, the theoretical data was verified using the Roboanalyzer software.

Aboti *et al*. [2] built a 5-DOF robotic arm prototype and used a SCARA configuration to pick and place a large number of components (Taper roller bearings) from a horizontal stack into a loading crate in an industrial setting. The study demonstrated the creation of a kinematic model, the creation of an inverse kinematic model, and the validation of forward kinematics using MATLAB. Denavit-Hartenberg parameters and a generalized algorithm were also used to develop the joint link parameters.

The numerical simulations of humanoid robot arm position control were conducted for both PID and non-linear PID controllers in [3]. For humanoid robot arms, the hardware implementation of nonlinear PID controllers was presented in this study. To confirm the simulation results, nonlinear PID control embedded hardware is used to perform experiments on humanoid robot arm control tasks. The experiments revealed the performance of the nonlinear PID controller's hardware design. Although noise was observed, the nonlinear PID controller performs much better than the PID controller.

Furthermore, Adar and Kozan [4] compared the performance of PID and 2-DOFPID controllers designed for controlling a 6-DOF robotic arm. It was discovered that the x, y position of 2-DOF PID had less overshoot and a faster settling time than PID. Even though the z position had limited movement in both controllers, the 2-DOF PID controller had fewer vibrations. The per cent error and total (RMS) error of a 2-DOF PID were lower. The authors showed that the 2-DOF PID controller outperformed the traditional PID controller.

Robotic arms with five degrees of freedom (DOF) were invented and built by Oluwajobi and Oridate [5]. The robotic arm can be reconfigured to perform a variety of tasks using servos and inverse kinematics. The authors demonstrated how the robotic arm could be useful in an industrial setting, particularly in the production, packaging, and mining industries.

There were three control methods presented by Khan *et al*. [6] for the control of a 6-DOF robotic arm for nuclear plant dismantling: PID, SMC, and SMC with sliding perturbation observer (SMCSPO). The Lagrange approach was used to model the system's dynamics. The trajectory for the manipulator's end-effector was done first, and then the trajectory for each joint was computed. Then, in MATLAB/Simulink,

Address correspondence to this article at the Department of Electrical/Electronic Engineering, Federal University of Petroleum Resources Effurun, Nigeria;
E-mail: nyongbassey.bassey@fupre.edu.ng

E-ISSN: 2409-9694/22

control algorithms were designed and implemented. The simulation results demonstrated that PID was a linear control; thus, when controlling a system with uncertainties, PID's performance was poor.

An anthropomorphic tele-robot system controlled and commanded by a tele-operator via the man-machine interface was studied and developed by Kumra *et al*. [7]. The authors presented a man-machine functionality built on a real robotic platform. The presented model of the robotic arm also included the correct joint angles for moving the arm gripper to any position and orientation within its workspace. The model's output was compared to the robot's actual performance in completing a task, such as a pick and place of an object and results showed ±0.5 cm precision was achieved by the robot.

The Parallel-Axis Theorem was utilized to predict the moment of inertia of the links in a robotic arm technique based on Gazebo [8]. The system's most important components are the joint controllers and the path planning algorithm. Because of its ease of hardware abstraction, a robot operating system (ROS) was chosen to organize task architecture. The simulation system can analyze and compare the responses of the robotic arm to different algorithms and target poses. When multiple targets were given at the same time, the system analyzed which is optimal in terms of path length and velocity change smoothness.

The Robotics Toolbox for MATLAB was demonstrated in a tutorial paper [9]. Many of the essential tools required for robotic modelling and simulation, as well as analyzing experimental results and teaching, were included in the Toolbox. The use of a single matrix to completely describe the kinematics and dynamics of any serial-link manipulator is an important feature. The use of a single matrix to completely describe the kinematics and dynamics of any serial-link manipulator is a key feature of the Toolbox. The Robotics Toolbox, in contrast to commercial robot simulation packages, was designed for research and education purposes.

The design of a robotic manipulator arm based on the Programmable Universal Manipulator Arm (PUMA560), but with various structural alterations, was detailed elsewhere [10]. The lengths of the links are changed to support the manipulator's different loading conditions. The PUMA560 robot has six degrees of freedom (DOF) and so all joints are revolute joints. The joint axes of joint 4, joint 5, and joint 6 have a specific intersection point for these robots.

This paper aims to present the modelling, kinematic analysis, and simulation results of an educational 6-DOF (Degrees of Freedom) robotic arm intended for welding oil and gas pipelines and other generic tasks in the MATLAB/Simulink-Simscape environment in a comprehensive way.

2. METHODOLOGY

This section describes the robotic design and modelling in the Simscape/Simulink environment as well as the formalization of the homogeneous transformation matrix (which describes) for the forward kinematics of the robot arm via the Denavit and Hartenberg (D-H) method.

2.1. 6 - DoF Robotic Arm Modelling

The robot from the Base to the End-Effector (EE) has five links L1-L6 in between six (6) revolute joints J1 – J6 which bestow upon it six degrees of freedom in which rotation can occur.

Furthermore, the six revolute joints are actuated using DC Servomotors which are widely used in

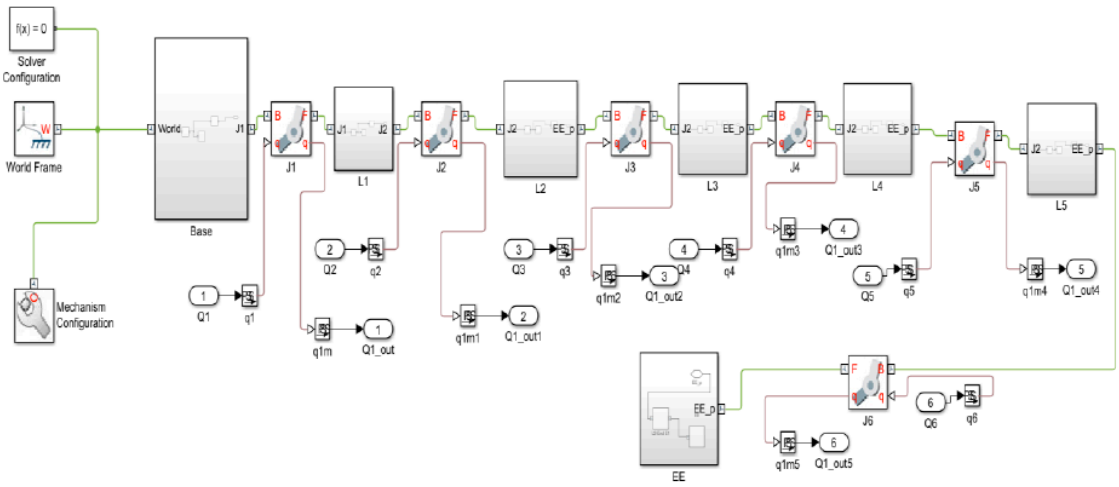

Figure 1: 6-DOF Robot Internal Architecture designed in Simscape/Simulink Environment.

robotics to provide precise control over angular position, velocity and acceleration and torque requirements. The DC Servo motor is used in combination with worm gears for locking in place the six revolute joints, magnetic encoders for sensing the angular position as well as a microcontroller which generates the pulse width modulated (PWM) necessary to precisely actuate for instance rotate a joint angle by 180-degree. In practice, the DC Servo motor selected for use must have sufficient torque to overcome the joint resistance [5]. Figure **1** shows the Robot's internal architecture in MATLAB/Simulink-Simscape Environment, while Figure **2**, shows the designed Robot Arm manipulator for Oil and Gas pipe welding and Table **1**, summarises the robot parameters and description.

2.2. Forward Kinematics

The kinematics analysis which describes the robotic structure is expressed mathematically using Denavit and Hartenberg (D-H) parameters. The D-H parameters presented in Table **2**, express the relationship between two joints via four parameters [5], [11], which consist of two angles in radians and link length in meters.

Note that, $LL1, LL4$ and $LL6$ in Table **2** denote the link length for $L1, L4$ and $L6$ respectively.

The general form of the homogeneous transformation matrix is presented in (1):

$$T_n^{n-1} = Rot(x, \alpha_{n-1})\ Trans(l_{n-1}, 0, 0)\ Rot(z, \theta_n)\ Trans(0, 0, d_n) \quad (1)$$

where,

$$Rot(x, \alpha_{n-1}) = \begin{bmatrix} 1 & 0 & 0 & 0 \\ 0 & C(\alpha_{n-1}) & -S(\alpha_{n-1}) & 0 \\ 0 & S(\alpha_{n-1}) & C(\alpha_{n-1}) & 0 \\ 0 & 0 & 0 & 1 \end{bmatrix} \quad (2)$$

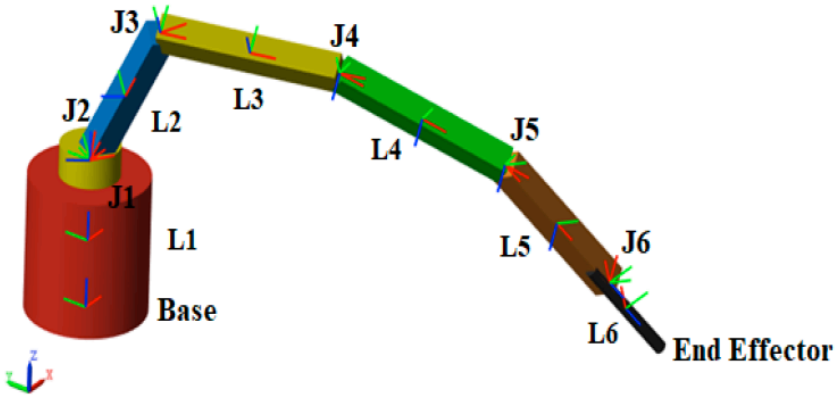

Figure 2: 6-DoF Robot arm for Oil and Gas Pipeline welding operations.

Table 1: Robot modelling Parameters

Robot Components/ Parameters	Description/Rating	Dimension	Geometry
J1-J6 PWM Controller	ATmega328P Micro-controller	-	-
J1-J6 Actuator	24 V 100 rpm 80W 8 N/m DC Reversible Worm Gear Motor	0.085 x 0.035 m	Cylinder (R x H)
J1-J6 Position (rad) Sensor	Magnetic Encoder	-	-
$L1$	Link between Robot Base and $J1$	0.05 x 0.1 m	Cylinder (R x H)
$L2$	Link between $J1$ and $J2$	0.025 x 0.025 m	Cylinder (R x H)
$L3$	Link between $J2$ and $J3$	0.15 x 0.02 x 0.02 m	Brick (L x B x H)
$L4$	Link between $J3$ and $J4$	0.15 x 0.02 x 0.02 m	Brick (L x B x H)
$L5$	Link between $J4$ and $J5$	0.15 x 0.02 x 0.02 m	Brick (L x B x H)
$L6$	Link between $J5$ and End Effector welding tool joint	0.05 x 0.1 m	Cylinder (R x H)
J1-J6	Revolute Joints	-	Cylindrical

Table 2: D-H Parameters for the Robotic Arm

Link Number	α_{n-1}(rad)	l_{n-1}(m)	θ_n(rad)	d_n(m)	Joint Angle Constraints
T_1^0	$\alpha_0 = \pi/2$	$l_0 = 0$	θ_1	$d_1 = LL1$	$-\pi \leq \theta_1 \leq \pi$
T_2^1	$\alpha_1 = 0$	$l_1 = 0$	θ_2	$d_2 = 0$	$-\pi/2 \leq \theta_2 \leq \pi/2$
T_3^2	$\alpha_2 = \pi/2$	$l_2 = 0$	θ_3	$d_3 = 0$	$-\pi/2 \leq \theta_3 \leq \pi/2$
T_4^3	$\alpha_3 = \pi/2$	$l_3 = 0$	θ_4	$d_4 = LL4$	$-\pi/2 \leq \theta_4 \leq \pi/2$
T_5^4	$\alpha_4 = \pi/2$	$l_4 = 0$	θ_5	$d_5 = 0$	$-\pi/2 \leq \theta_5 \leq \pi/2$
T_6^5	$\alpha_5 = 0$	$l_5 = 0$	θ_6	$d_6 = LL6$	$-3/4\pi \leq \theta_6 \leq 3/4\pi$

$$Rot(z,\theta_n) = \begin{bmatrix} C(\theta_n) & -S(\theta_n) & 0 & 0 \\ S(\theta_n) & C(\theta_n) & 0 & 0 \\ 0 & 0 & 1 & 0 \\ 0 & 0 & 0 & 1 \end{bmatrix} \quad (3)$$

$$Trans(l_{n-1},0,0) = \begin{bmatrix} 1 & 0 & 0 & l_{n-1} \\ 0 & 1 & 0 & 0 \\ 0 & 0 & 1 & 0 \\ 0 & 0 & 0 & 1 \end{bmatrix} \quad (4)$$

$$Trans(0,0,d_n) = \begin{bmatrix} 1 & 0 & 0 & 0 \\ 0 & 1 & 0 & 0 \\ 0 & 0 & 1 & d_{n-1} \\ 0 & 0 & 0 & 1 \end{bmatrix} \quad (5)$$

Note that, C and S are used in all the matrix equations and denote Cos and Sine trigonometric functions respectively. Also, $L1, L4$ and $L6$ will now be used for conciseness to represent the corresponding link lengths $LL1, LL2$ and $LL6$ respectively in the equations.

Therefore, the homogeneous transformation matrix for the forward kinematics of the robotic arm derived via Table **2** is as follows:

$$T_1^0 = Rot\left(x,\frac{\pi}{2}\right) Rot(z,\theta_1) Trans(0,0,L1) \quad (6)$$

$$T_2^1 = Rot(Z,\theta_2) \quad (7)$$

$$T_3^2 = Rot(x,\pi/2) Rot(z,\theta_3) \quad (8)$$

$$T_4^3 = Rot\left(x,\frac{\pi}{2}\right) Rot(z,\theta_4) Trans(0,0,L4) \quad (9)$$

$$T_5^4 = Rot(x,\pi/2) Rot(z,\theta_5) \quad (10)$$

$$T_6^5 = Rot(z,\theta_6) Trans(0,0,L6) \quad (11)$$

The homogeneous transformation matrix is of the general form

$$T_N^R = \begin{bmatrix} R_B^A & Trans \\ 0_{1x3} & 1 \end{bmatrix} = \begin{bmatrix} x_x & y_x & z_x & P_x \\ x_y & y_y & z_y & P_y \\ x_z & y_z & z_z & P_z \\ 0 & 0 & 0 & 1 \end{bmatrix} \quad (12)$$

Therefore, the forward kinematics homogeneous transformation from the Base reference frame to the End effector (EE) T_6^0 is expressed as follows:

$$T_6^0 = T_1^0\, T_2^1\, T_3^2\, T_4^3\, T_5^4\, T_6^5 = \begin{bmatrix} C(\theta_n) & -S(\theta_n) & 0 & 0 \\ S(\theta_n) & C(\theta_n) & 0 & 0 \\ 0 & 0 & 1 & 0 \\ 0 & 0 & 0 & 1 \end{bmatrix} \quad (13)$$

$$T_1^0 = \begin{bmatrix} C(\theta_1) & -S(\theta_1) & 0 & 0 \\ 0 & 0 & -1 & -L1 \\ S(\theta_1) & C(\theta_1) & 0 & 0 \\ 0 & 0 & 0 & 1 \end{bmatrix},$$

$$T_2^1 = \begin{bmatrix} C(\theta_2) & -S(\theta_2) & 0 & 0 \\ S(\theta_2) & C(\theta_2) & 0 & 0 \\ 0 & 0 & 1 & 0 \\ 0 & 0 & 0 & 1 \end{bmatrix}$$

$$T_3^2 = \begin{bmatrix} C(\theta_3) & -S(\theta_3) & 0 & 0 \\ 0 & 0 & -1 & 0 \\ S(\theta_3) & C(\theta_3) & 0 & 0 \\ 0 & 0 & 0 & 1 \end{bmatrix},$$

$$T_4^3 = \begin{bmatrix} C(\theta_4) & -S(\theta_4) & 0 & 0 \\ 0 & 0 & -1 & L4 \\ S(\theta_4) & C(\theta_4) & 0 & 0 \\ 0 & 0 & 0 & 1 \end{bmatrix}$$

$$T_5^4 = \begin{bmatrix} C(\theta_5) & -S(\theta_5) & 0 & 0 \\ 0 & 0 & -1 & 0 \\ S(\theta_5) & C(\theta_5) & 0 & 0 \\ 0 & 0 & 0 & 1 \end{bmatrix},$$

$$T_6^5 = \begin{bmatrix} C(\theta_6) & -S(\theta_6) & 0 & 0 \\ S(\theta_6) & C(\theta_6) & 0 & 0 \\ 0 & 0 & 1 & L6 \\ 0 & 0 & 0 & 1 \end{bmatrix} \quad (14)$$

Base to End-Effector transformation matrix is of the general form

$$T_6^0 \equiv \begin{bmatrix} x_x & y_x & z_x & P_x \\ x_y & y_y & z_y & P_y \\ x_z & y_z & z_z & P_z \\ 0 & 0 & 0 & 1 \end{bmatrix} \quad (15)$$

Where the transformation matrix for specific rotation of the EE to the Base reference frame of the robot in 3-dimensional Euclidean space $\{[\boldsymbol{x_x, x_y, x_z}]^T, \{[\boldsymbol{y_x, y_y, y_z}]^T, \{[\boldsymbol{z_x, z_y, z_z}]^T\}$ is given as follows:

$$\boldsymbol{x_x} = C\theta_6\big(C\theta_5C\theta_4C\theta_3(C\theta_1C\theta_2 - S\theta_1S\theta_2) - S\theta_5S\theta_3(C\theta_1S\theta_2 + S\theta_1C\theta_2)\big) - S\theta_6\big(S\theta_5C\theta_4C\theta_3(C\theta_1C\theta_2 - S\theta_1S\theta_2) - S\theta_5S\theta_3(C\theta_1S\theta_2 + S\theta_1C\theta_2)\big) \quad (16)$$

$$\boldsymbol{x_y} = C\theta_6(C\theta_5C\theta_4S\theta_3 + S\theta_5C\theta_3) + S\theta_6(S\theta_5C\theta_4S\theta_3 + C\theta_5C\theta_3) \quad (17)$$

$$\boldsymbol{x_z} = C\theta_6\big(C\theta_5C\theta_4C\theta_3(S\theta_1C\theta_2 + C\theta_1S\theta_2) + S\theta_5S\theta_3(S\theta_1C\theta_2 + C\theta_1S\theta_2)\big) + S\theta_6S\theta_5C\theta_4C\theta_3(S\theta_1C\theta_2 - C\theta_1S\theta_2) \quad (18)$$

$$\boldsymbol{y_x} = S\theta_6\big(C\theta_5C\theta_4C\theta_3(C\theta_1C\theta_2 - S\theta_1S\theta_2) - S\theta_5S\theta_3(C\theta_1S\theta_2 + S\theta_1C\theta_2)\big) + C\theta_6\big(S\theta_5C\theta_4C\theta_3(C\theta_1C\theta_2 + S\theta_1S\theta_2) - C\theta_5S\theta_3(C\theta_1S\theta_2 + S\theta_1C\theta_2)\big) \quad (19)$$

$$\boldsymbol{y_y} = -S\theta_6(C\theta_6C\theta_5C\theta_4S\theta_3 + S\theta_5C\theta_3) + C\theta_6(S\theta_5C\theta_4S\theta_3 + C\theta_5C\theta_3)$$

$$\boldsymbol{y_z} = -S\theta_6\big(C\theta_5C\theta_4C\theta_3(S\theta_1C\theta_2 + C\theta_1S\theta_2) + S\theta_5S\theta_3(S\theta_1C\theta_2 + C\theta_1S\theta_2)\big) + C\theta_6S\theta_5C\theta_4C\theta_3(S\theta_1C\theta_2 + C\theta_1S\theta_2) \quad (20)$$

$$\boldsymbol{z_x} = S\theta_3(C\theta_1S\theta_2 + S\theta_1C\theta_2) \quad (21)$$

$$\boldsymbol{z_y} = -C\theta_3 \quad (22)$$

$$\boldsymbol{z_z} = S\theta_4C\theta_3(S\theta_1C\theta_2 + C\theta_1S\theta_2) \quad (23)$$

The transformation matrix specific displacement of the EE to the Base reference frame of the robot in 3-dimensional Euclidean space $\{\boldsymbol{P_x}, \boldsymbol{P_y}, \boldsymbol{P_z}\}$ is given as follows:

$$\boldsymbol{P_x} = L6S\theta_3(C\theta_1S\theta_2 + S\theta_1C\theta_2) + L4S\theta_3(C\theta_1S\theta_2 + S\theta_1C\theta_2) \quad (24)$$

$$\boldsymbol{P_y} = -(L6C\theta_3 + L4C\theta_3 + L1) \quad (25)$$

$$\boldsymbol{P_z} = L6S\theta_4C\theta_3(C\theta_1S\theta_2 + S\theta_1C\theta_2) - L4S\theta_3(C\theta_1S\theta_2 + S\theta_1C\theta_2) \quad (26)$$

Furthermore, the mathematical relationship which describes the End-Effector pose or position with regards to the world frame or Base frame of the 6 DoF Robot in Figure **3** in terms of $[X, Y]$ cartesian plane coordinates using the Cosine trigonometric law is as follows:

$$X^2 = (L3 + L4 + L5 + L6)^2 + (L1 + L2)^2 - 2L1L2(L3(\theta_2 - \theta_3) + L4C(\theta_2 - (\theta_3 + \theta_4)) + L5C(\theta_2 - (\theta_3 + \theta_4 - \theta_5)) + L6C(\theta_2 - (\theta_3 + \theta_4 - \theta_5))C(\theta_2 - \theta_3) \quad (27)$$

The horizontal coordinate of the End-Effector is obtained as follows:

$$X = (L3 + L4 + L5 + L6) + (L1 + L2) - \sqrt{\begin{matrix}2L1L2(L3(\theta_2 - \theta_3) + L4C((\theta_2 - (\theta_3 + \theta_4)) + L5C((\theta_2 - (\theta_3 + \theta_4 - \theta_5)) \\ +L6C(\theta_2 - (\theta_3 + \theta_4 - \theta_5))C(\theta_2 - \theta_3)\end{matrix}} \quad (28)$$

To determine the vertical height of the angle of interception (triangle E D $\hat{F}$) between the $[X, Y]$ coordinate of the Robot's Base and End Effector is as follows

$$\angle(F) = -C^{-1}([X + (L3 + L4 + L5 + L6)^2 - (L1 + L2)^2]/2X(L3 + L4 + L5 + L6)^2) \quad (29)$$

The vertical coordinate of the End-Effector by inspection coincides with the origin of $L1$,

$$Y = 0 \quad (30)$$

3. SIMULATION RESULT AND DISCUSSION

The forward kinematics simulation of the robotic arm was modelled in a Simulink-Simscape environment as shown in Figure **4**.

The simulation which lasted for 10s illustrates the motion or forward kinematics of the robotic arm to the Base reference frame and End effector tool piece, with

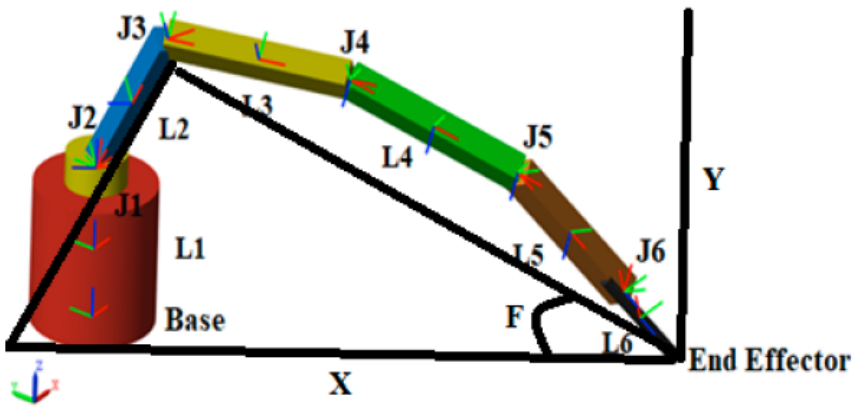

Figure 3: 6-DoF Robot geometrical analysis for Inverse Kinematics.

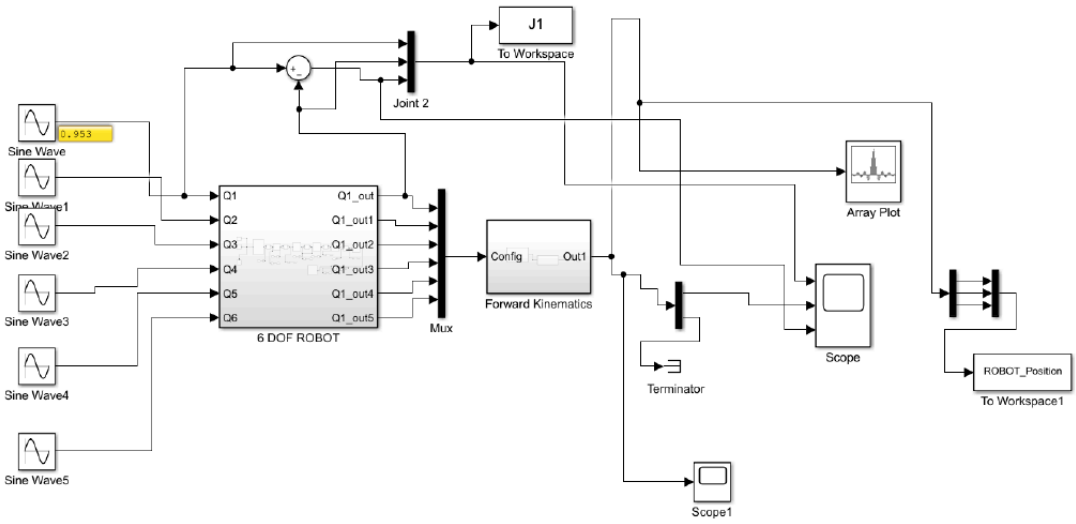

Figure 4: 6 -DOF Robot Forward Kinematics Simulation Model.

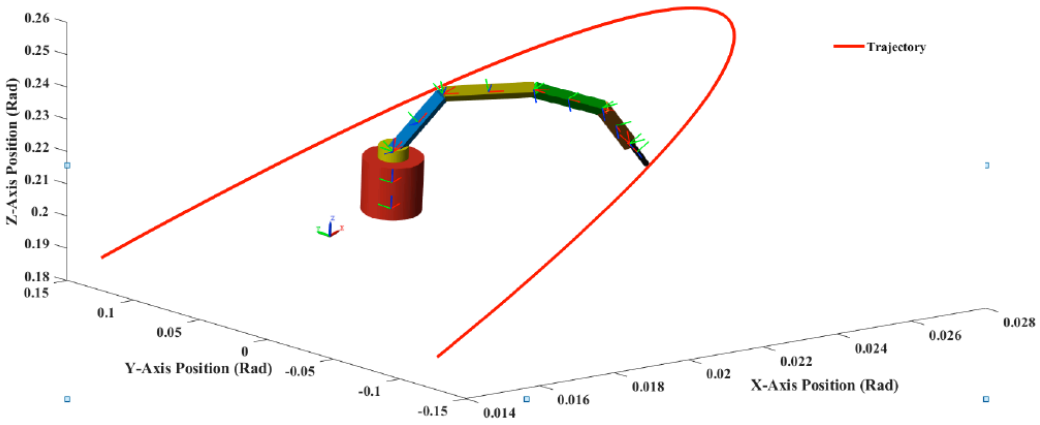

Figure 5: Robot arm End-Effector performing elliptical welding.

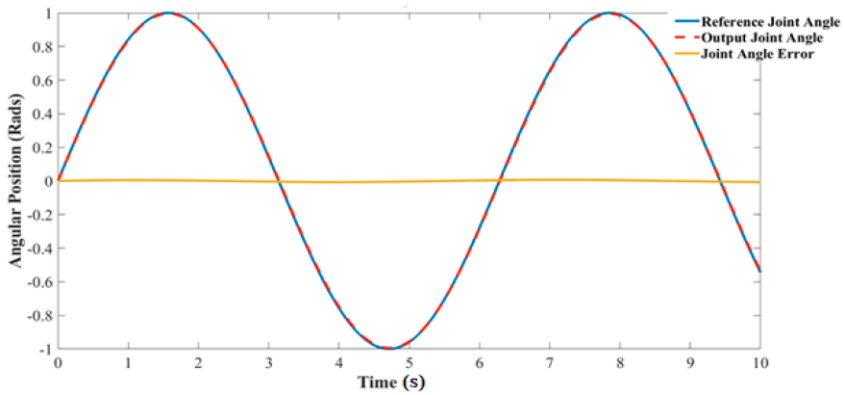

Figure 6: Robot Arm Joint Angle 1 Reference and Output response.

each of the six joint angles, which were actuated using sinusoidal references. The results as shown in Figure **5**, clearly show the End-Effector tracing an elliptical path a conditional constraint which would be required for the welding operation. Furthermore, the reference joint angles and the corresponding actuated joint angles were in good agreement with no overshoot observed as shown in Figure **6**.

CONCLUSION

This paper modelled and simulated a 6-DoF Robotic arm for welding oil and gas pipelines. Moreso, the model was developed, analyzed analytically and simulated in MATLAB/SIMULINK environment for educational purposes. The simulation results showed that the robot can perform without overshooting an

elliptical reference path in a 3-dimensional space, an important condition which must be met to weld cylindrical oil and gas pipelines. Future work will use an optimisation algorithm to solve the inverse kinematics joint angles for a given pose of the End-Effector.

REFERENCES

[1] MH. Ali, Y. Kuralbay, A. Aitmaganbet, and MAS. Kamal, “Design of a 6-DOF robot manipulator for 3D printed construction”. Materials Today: Proceedings, 2022; 49: 1462-1468. https://doi.org/10.1016/j.matpr.2021.07.228

[2] A. Aboti, S. Acharya, A. Anand, R. Chintale, and V. Ruiwale, “Design of a Prototype of a Pick and Place Robotic Arm”. International Journal of Engineering Science and Innovative Technology, 2016; 5(3): 74-81.

[3] JS. Kim, HW. Jeon, and S. Jung, “Hardware implementation of nonlinear PID controller with FPGA based on floating point operation for 6-DOF manipulator robot arm”. In International Conference on Control, Automation and Systems, 2007; 1066-1071.

[4] NG Adar, and R. Kozan, "Comparison between real-time PID and 2-DOF PID controller for 6-DOF robot arm." Acta Physica Polonica A, 2016; 130(1): 269-271. https://doi.org/10.12693/APhysPolA.130.269

[5] OA. Oluwajobi, and AA. Oridate, "Design and Development of an Educational 5-DoF Robotic Arm." International Journal of Robotics and Automation, 2019; 6: 55-65. https://doi.org/10.31875/2409-9694.2019.06.7

[6] H. Khan, SJ. Abbasi, KD. Kallu, and MC. Lee, "Robust control design of 6-DOF robot for nuclear power plant dismantling." In International Conference on Robotics and Automation in Industry (ICRAI), 2019; pp. 1-7. https://doi.org/10.1109/ICRAI47710.2019.8967383

[7] S. Kumra, R. Saxena, and S. Mehta, "Design and development of 6-DOF robotic arm controlled by Man Machine Interface." In IEEE International Conference on Computational Intelligence and Computing Research, 2012; pp. 1-5. https://doi.org/10.1109/ICCIC.2012.6510243

[8] Z. Huang, F. Li, and L. Xu, "Modeling and simulation of 6 DOF robotic arm based on gazebo." In 6th International Conference on Control, Automation and Robotics (ICCAR), 2020; pp. 319-323. https://doi.org/10.1109/ICCAR49639.2020.9107989

[9] PI. Corke, "A robotics toolbox for MATLAB." IEEE Robotics & Automation Magazine, 1996; 3(1): 24-32. https://doi.org/10.1109/100.486658

[10] A. Khan, and WL. Quan, "Structure design and workspace calculation of 6-DOF underwater manipulator." In 14th International Bhurban Conference on Applied Sciences and Technology (IBCAST), 2017; pp. 651-655. https://doi.org/10.1109/IBCAST.2017.7868119

[11] J. Denavit, and RS. Hartenberg. “A kinematic notation for lower-pair mechanisms based on matrices.” ASME J. Appl. Mech., 1955; pp. 215-221. https://doi.org/10.1115/1.4011045

Received on 20-03-2022 Accepted on 29-04-2022 Published on 15-05-2022

DOI: https://doi.org/10.31875/2409-9694.2022.09.1